informa
healthcare

ORIGINAL ARTICLE

Adair-based hemoglobin equilibrium with oxygen, carbon dioxide and hydrogen ion activity

MAREK MATEJÁK, TOMÁŠ KULHÁNEK & STANISLAV MATOUŠEK

The Institute of Pathological Physiology, First Faculty of Medicine, Charles University in Prague, Czech Republic

Abstract

As has been known for over a century, oxygen binding onto hemoglobin is influenced by the activity of hydrogen ions (H^+), as well as the concentration of carbon dioxide (CO_2). As is also known, the binding of both CO_2 and H^+ on terminal valine-1 residues is competitive. One-parametric situations of these hemoglobin equilibria at specific levels of H^+, O_2 or CO_2 are also well described. However, we think interpolating or extrapolating this knowledge into an 'empirical' function of three independent variables has not yet been completely satisfactory. We present a model that integrates three orthogonal views of hemoglobin oxygenation, titration, and carbamination at different temperatures. The model is based only on chemical principles, Adair's oxygenation steps and Van't Hoff equation of temperature dependences. Our model fits the measurements of the Haldane coefficient and CO_2 hemoglobin saturation. It also fits the oxygen dissociation curve influenced by simultaneous changes in H^+, CO_2 and O_2, which makes it a strong candidate for integration into more complex models of blood acid-base with gas transport, where any combination of mentioned substances can appear.

Key Words: *Acid-base equilibrium, blood gas analysis, carboxyhemoglobin, hemoglobin A, oxyhemoglobins*

Abbreviations: ODC, hemoglobin oxygen dissociation curve; 2,3-DPG, 2,3-diphosphoglycerate; [X], molar concentration of X in $mol.m^{-3}$; aH^+, activity of hydrogen ions, where $pH = -\log_{10}(aH^+)$; αO_2, O_2 solubility in $mol.m^{-3}.Pa^{-1}$; αCO_2, CO_2 solubility in $mol.m^{-3}.Pa^{-1}$; pO_2, partial pressure of O_2 in Pa; pCO_2, partial pressure of CO_2 in Pa; Hb_u, hemoglobin alpha or beta subunit; Hb_{uD}, deoxygenated Hb_u; Hb_{uO}, oxygenated Hb_u; $Hb_uNH_3^+$, Hb_u with protonated Nterminus; $Hb_{uD}NH_3^+$, Hb_{uD} with protonated Nterminus; $Hb_{uO}NH_3^+$, Hb_{uO} with protonated Nterminus; Hb_uNH_2, Hb_u with $-NH_2$ form of Nterminus; $Hb_{uD}NH_2$, Hb_{uD} with $-NH_2$ form of Nterminus; $Hb_{uO}NH_2$, Hb_{uO} with $-NH_2$ form of Nterminus; Hb_uCOO^-, Hb_u with carboxylated Nterminus; $Hb_{uD}COO^-$, Hb_{uD} with carboxylated Nterminus; $Hb_{uO}COO^-$, Hb_{uO} with carboxylated Nterminus; Hb_uAH, Hb_u with protonated side-chains; $Hb_{uD}AH$, Hb_{uD} with protonated side-chains; $Hb_{uO}AH$, Hb_{uO} with protonated side-chains; Hb_uA^-, Hb_u with deprotonated side-chains; $Hb_{uD}A^-$, Hb_{uD} with deprotonated side-chains; $Hb_{uO}A^-$, Hb_{uO} with deprotonated side-chains; $Hb_uA^-NH_2$, selected normalized form of Hb_u with deprotonated side-chains and NH_2 form of Nterminus; $Hb_{uD}A^-NH_2$, deoxygenated form of $Hb_uA^-NH_2$; $Hb_{uO}A^-NH_2$, oxygenated form of $Hb_uA^-NH_2$; f_{nD}, fraction of $Hb_{uD}A^-NH_2$ from Hb_{uD}; f_{nO}, fraction of $Hb_{uO}A^-NH_2$ from Hb_{uO}; f_{zcD}, fraction of $Hb_{uD}NH_2$ form Hb_{uD}; f_{zcO}, fraction of $Hb_{uO}NH_2$ form Hb_{uO}; f_{hD}, fraction of $Hb_{uD}A^-$ form Hb_{uD}; f_{hO}, fraction of $Hb_{uO}A^-$ form Hb_{uO}; $\Delta H+_h$, change of valence (charge) on side-chains during deoxygenation per one Hb_u; $\Delta H+_z$, protonation of $-NH_2$ form of Nterminus during deoxygenation per one Hb_u; $\Delta H+_c$, decarboxylation of carboxylated Nterminus during deoxygenation per one Hb_u; ΔH^+, Haldane coefficient per hemoglobin subunit; Hb_t, hemoglobin tetramer without bound O_2 molecules; $(O_2)_iHb_t$, hemoglobin tetramer with the number of i bound O_2 molecules; $(O_2)_iHb_{tn}$, hemoglobin tetramer composed only of $Hb_uA^-NH_2$ subunit forms with the number of i bound O_2 molecules; sO_2, O_2 saturation of hemoglobin; sCO_{2D}, CO_2 saturation of deoxyhemoglobin; sCO_{2O}, CO_2 saturation of oxyhemoglobin; sCO_2, CO_2 saturation of hemoglobin; tCO_2, total concentration of CO_2 = free dissolved $CO_{2+} + HCO_3^- + CO_3^{2-} + Hb_uCOO^-$; dTH, shift of titration curve with the change of both pO_2 and pCO_2 to zero, which equals to how many moles of strong acid must be added to one mole of Hb_u to reach the pH of the chosen standard titration curve (O_2 and CO_2 free); pH, acidity/basicity of hemoglobin solution (e.g. inside erythrocytes); pH_p, pH in plasma (e.g. acidity/basicity of blood).

Correspondence: Marek Mateják, U Nemocnice 5, Prague 2, 128 53, Czech Republic. Tel: + 420 776 301 395. Fax: + 420 224 965 916. E-mail: marek.matejak@lf1.cuni.cz

RIGHTS LINK

Introduction

Human hemoglobin A is one of the most extensively studied protein macromolecules. The composition and 3D conformation of both α and β chains is known [1,2] and the binding of O_2, H^+ and 2,3-DPG has been described [2,3]. Since the 1930s it has generally been believed that CO_2 binding to Hb occurs by carbamination of the amino-terminus, i.e. forming a carboxylate compound [4–6]. This hemoglobin carbamination was verified by Morrow et al. [7], who used nuclear magnetic resonance of $^{13}CO_2$ to find its exact binding sites at valine-1. The shift of titration between oxygenated and deoxygenated forms is also well known. Called the Bohr or Haldane effect [8–10], it is caused by the same valine-1 side and by more than 10 other acid-base residues [2,11].

The most common descriptions of the hemoglobin oxygen dissociation curve (ODC) are the allosteric models [12,13], the model based on Hill equation [14,15], and Adair's four-step model [16]. Some of the ODC models [15,17,18] also include the effects of varying pH and CO_2 concentration. However, these models operate only with interpolation or extrapolation of ODC from normal pH or normal pCO_2 and do not take into account the chemical dependences between titration [8] and carbamination [19]. They fail when both pH and CO_2 are not at normal values, especially in the alkaline pH range.

Based on these findings, we propose a hemoglobin binding equilibrium model that starts with a description of hemoglobin-oxygen dissociation using a slightly modified version of Adair's approach [16]. We continue by describing the relationship between CO_2 and H^+ as competitive inhibition in the amino group of terminal valine-1 residue on each chain (suffixes *z* and *c*), which is in accordance with the known facts [4,6,20]. Finally, we lump all other acid-base side chains residues in a hemoglobin subunit into one Bohr proton-binding site of the side chain residues. These are denoted by the suffix *h* in the article.

Methods

The model is built in Mathematica 9.0 (Wolfram, Champaign, IL, USA) and also in Dymola FD01 2014 (Dassault Systemes, Paris, France) as an example of chemical package in open-source Modelica library Physiolibrary 2.2.0 (http://www.physiolibrary.org) [21,22] according to the model structure defined in the following section. The model contains only physiological parameters such as gas solubilities and dissociation coefficients of defined reactions. The unknown parameters are fitted to the data of Siggaard-Andersen [23], Bauer and Schröder [24], Severinghaus [18], Matthew et al. [1] and Reeves [25]

using Mathematica function FindFit and also using parameter estimation method suggested by Kulhanek et al. [26].
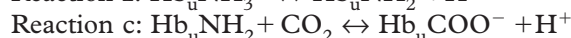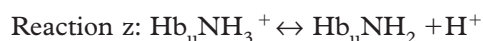
Free dissolved concentrations of $[O_2]$ and $[CO_2]$ in red blood cells are calculated from gas partial pressures using Henry's law ($[O_2] = \alpha O_2 * pO_2$ and $[CO_2] = \alpha CO_2 * pCO_2$) with solubility coefficients $\alpha O_2 = 1.005*10^5$ mol.m^{-3}.Pa^{-1} measured at 38°C by Sendroy et al. [27], and $\alpha CO_2 = 2.3*10^4$ mol.m^{-3}.Pa^{-1} at 37°C, as proposed by Maas et al. [28]. These solubilities are slightly different from solubilities in pure water or in plasma because of the effects of salts and proteins inside erythrocyte [27].

Model structure

The model is built upon several simplifying assumptions. Firstly, each of four hemoglobin tetramer subunits is treated as identical, even though (slight) differences are known to exist between α and β subunits. Secondly, CO_2 or H^+ binding is supposed not to affect the CO_2 or H^+ affinities in the other three subunits. Thus, the interaction between the subunits is modeled purely through the varying affinities of oxygen in each oxygenation step. The third simplifying assumption has already been mentioned; it is lumping all Bohr proton binding sites of subunit into two (first for the valine-1 amino-terminus and second for the side chains residues), a simplification first suggested by Antonini [29].

Model structure of hemoglobin subunit

The three reactions that participate in the Bohr and Haldane effect of each subunit are as follows:

Reaction z: $Hb_u NH_3^+ \leftrightarrow Hb_u NH_2 + H^+$
Reaction c: $Hb_u NH_2 + CO_2 \leftrightarrow Hb_u COO^- + H^+$
Reaction h: $Hb_u AH \leftrightarrow Hb_u A^- + H^+$

where the reactions z and c are competitive on the valine-1 amino-terminus, and the reaction h is independent of z or c.

The chemical equilibrium equations of these three reactions are Equations 1–3, where K_x is the equilibrium dissociation coefficients of the reaction *x* (i.e. *z*, *c* or *h*).

$$\text{Reaction z: } K_z = \frac{[Hb_u NH_2] * aH^+}{[Hb_u NH_3^+]} \quad (1)$$

$$\text{Reaction c: } K_c = \frac{[Hb_u COO^-] * aH^+}{[CO_2][Hb_u NH_2]} \quad (2)$$

$$\text{Reaction h: } K_h = \frac{[Hb_u A^-] * aH^+}{[Hb_u AH]} \quad (3)$$

These dissociation coefficients are different between oxy and deoxy subunits, which are distinguished by the subscripts O and D in the following text. They can be also written in their logarithmic

form, where $\mathbf{pK_x}$ means $-\log_{10}(K_x)$. Thus, for instance, pK_{zO} denotes the equilibrium coefficient of the reaction z for the oxy form of the hemoglobin subunit. Similar notation is used for describing the activity of hydrogen ions (acidity), where $pH = -\log_{10}$ (aH^+).

Using Equations 1–3 it is possible to express fractions of chosen species for deoxy and oxy subunits. We label these fractions as follows: Hb_uNH_2 fractions are called $\mathbf{f_{zD}}$ ($\mathbf{f_{zO}}$), Hb_uA^- fractions $\mathbf{f_{hD}}$ ($\mathbf{f_{hO}}$), $Hb_uA^-NH_2$ fractions $\mathbf{fn_D}$ ($\mathbf{fn_O}$) and Hb_uCOO^- fractions $\mathbf{sCO_{2D}}$ ($\mathbf{sCO_{2O}}$) as in Equation 4–7. The selection of form $Hb_uA^-NH_2$ from the orthogonal division into Hb_uNH_2 and Hb_uA^- is also illustrated in Figure 1A, B.

$$f_{zcD} = \frac{[Hb_{uD}NH_2]}{[Hb_{uD}]} = \frac{1}{1+10^{pKzD-pH}+[CO_2]10^{pH-pKcD}} \quad (4)$$

$$f_{hD} = \frac{[Hb_{uD}A^-]}{[Hb_{uD}]} = \frac{1}{10^{pKhD-pH}+1} \quad (5)$$

$$f_{nD} = \frac{[Hb_{uD}A^-NH_2]}{[Hb_{uD}]} = f_{zcD} \times f_{hD} \quad (6)$$

$$sCO_{2D} = \frac{[Hb_{uD}COO^-]}{[Hb_{uD}]} = 10^{pH-pKcD} f_{zcD}[CO_2] \quad (7)$$

We define a titration shift as the amount of acid that must be added to achieve the same pH after full

deoxygenation of the hemoglobin subunit. This change of subunit charge during deoxygenation (by the Bohr protons) is also called Haldane coefficient ΔH^+. The coefficient can be divided into contributions of the previously mentioned reactions ΔH^+_h, ΔH^+_z and ΔH^+_c, as is algebraically expressed by Equations 8–11.

$$\Delta H^+_h = -\frac{[Hb_{uD}A^-]-[Hb_{uO}A^-]}{[Hb_u]} = -(f_{hD}-f_{ho}) \quad (8)$$

$$\Delta H^+_z = \frac{[Hb_{uD}NH_3^+]-[Hb_{uo}NH_3^+]}{[Hb_u]}$$
$$= \left(\frac{10^{pKzD}}{10^{pH}}f_{zcD}-\frac{10^{pKzO}}{10^{pH}}f_{zcO}\right) \quad (9)$$

$$\Delta H^+_c = -\frac{[Hb_{uD}COO^-]-[Hb_{uO}COO^-]}{[Hb_u]}$$
$$= -(sCO_{2D}-sCO_{2O}) \quad (10)$$

$$\Delta H^+ = \Delta H^+_z + \Delta H^+_c + \Delta H^+_h \quad (11)$$

Model structure of hemoglobin tetramer

Chemical speciation of the hemoglobin tetramer molecule can be considered at various levels of detail; the one chosen as appropriate in our approach is indicated in Figure 1C. The possible forms include different combinations of oxygenated and deoxygenated
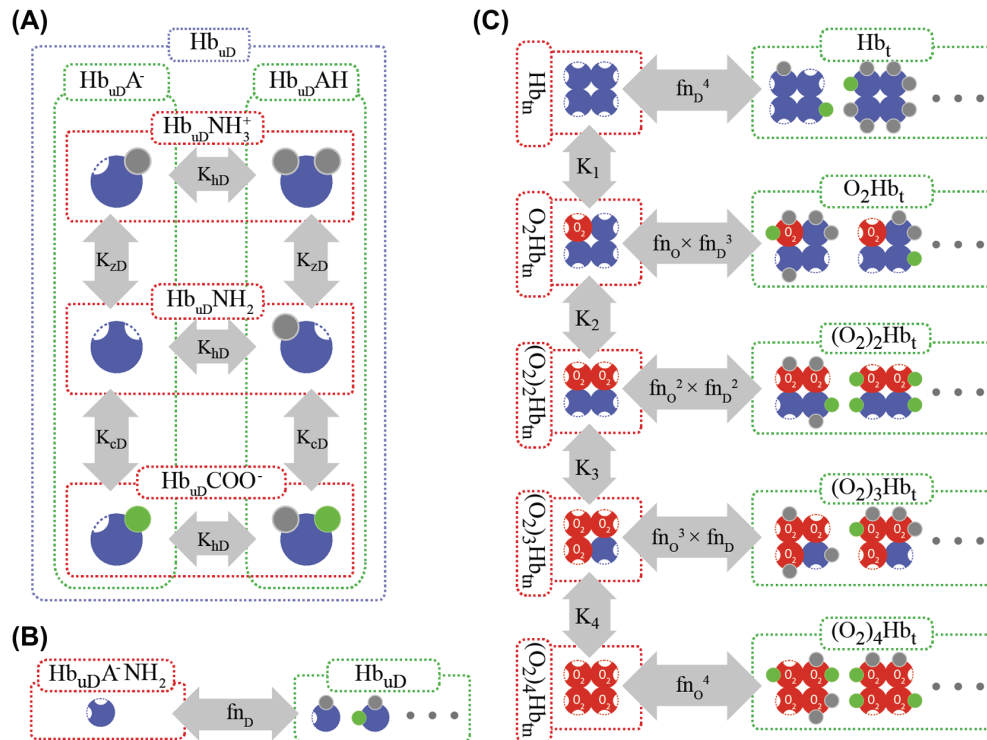
Figure 1. Schema of hemoglobin calculation. (A) Possible forms of deoxyhemoglobin subunit (the blue circles). The gray circles represent hydrogen ions, and the green circles represent carbon dioxide. The arrows with dissociation coefficients represent the reactions z, c and h. (B) Schema of chemical speciation of deoxyhemoglobin subunit. (C) Schema of chemical speciation and Adair's oxygenation steps of hemoglobin tetramer. This Figure is reproduced in color in the online version of *The Scandinavian Journal of Clinical & Laboratory Investigation*.

hemes, protonated and deprotonated oxygen-linked acid groups, and free or carboxylated amino endings of each chain. Yet because of the law of detailed balance in equilibrium [30], it is not necessary to calculate all reactions between these forms. As a result, only four oxygenation reactions need be selected for the calculation. This is done in accordance with Figure 1C, by selecting a tetramer form $(O_2)_i Hb_{tn}$ composed only of four subunits in the form $Hb_u A^- NH_2$ (H^+ and CO_2 free), and modeling oxygen binding to these forms with Adair-type coefficients of the following reactions:

$$O_2 Hb_{tn} \leftrightarrow Hb_{tn} + O_2$$
$$(O_2)_2 Hb_{tn} \leftrightarrow O_2 Hb_{tn} + O_2$$
$$(O_2)_3 Hb_{tn} \leftrightarrow (O_2)_2 Hb_{tn} + O_2$$
$$(O_2)_4 Hb_{tn} \leftrightarrow (O_2)_3 Hb_{tn} + O_2$$
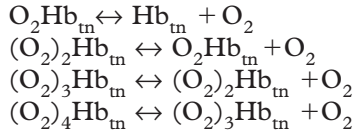
where dissociation coefficients are defined by Equation 12, which are also represented by vertical arrows at Figure 1C.

$$K_i = \frac{[(O_2)_{i-1} Hb_{tn}] \cdot [O_2]}{[(O_2)_i Hb_{tn}]} \quad (12)$$

For the next calculation, all forms can be expressed as a fraction of the deoxy-tetramer form $(O_2)_0 Hb_{tn}$, as shown in Equation 13.

$$[(O_2)_i Hb_{tn}] = \frac{[(O_2)_0 Hb_{tn}] \cdot [O_2]^i}{\prod_{j=1}^{i} K_i} \quad (13)$$

Let us move the attention from specific forms of Hb_{tn} to the description of the equilibrium within the whole group of Hb_t. Looking at Figure 1C, one can see that for each oxygenation step we can calculate the equilibrium in each horizontal line using Equation 14.

$$[(O_2)_i Hb_t] \cdot fn_D^{4-i} \cdot fn_O^i = [(O_2)_i Hb_{tn}] \quad (14)$$

The CO_2- and pH-dependent oxygen saturation equation in the Adair style (Equation 15) is algebraically derived from Equation 13–14, where $a_i = \frac{1}{\left(\prod_{j=1}^{i} K_j\right)}$
$x = (fn_D(pH, [CO_2]) / fn_O(pH, [CO_2])) * [O_2]$.

$$sO_2 = \frac{a_1 x + 2 a_2 x^2 + 3 a_3 x^3 + 4 a_4 x^4}{4 + 4 a_1 x + 4 a_2 x^2 + 4 a_3 x^3 + 4 a_4 x^4} \quad (15)$$

Hemoglobin saturation with CO_2 (sCO_2) is calculated separately in oxygenated and deoxygenated subunits forms (sCO_{2O} and sCO_{2D}) using Equation 16.

$$sCO_2 = sO_2 \cdot sCO_{2O} + (1 - sO_2) \cdot sCO_{2D} \quad (16)$$

Finally, the shift of titration after deoxygenation and decarbamination of the hemoglobin subunit can be expressed by Equation 17.

$$dTH = sO_2 \cdot \Delta H^+ + sCO_{2D} + \frac{sCO_{2D}}{1 + 10^{pH - pKzD}} \quad (17)$$

Temperature dependences

The temperature dependences are integrated using the Van't Hoff equation (Equation 18), where $R = 8.314$ $J.K^{-1}.mol^{-1}$ is gas constant, ΔH^θ is the standard enthalpy change, i.e. an amount of heat consumed by a reaction changing one mole of substrates to products, and K_2 and K_1 are Henry's coefficients of solution or the dissociation coefficient of the chemical reaction at temperature T_2 and T_1 (expressed in Kelvin).

$$\ln\left(\frac{K_2}{K_1}\right) = \frac{-\Delta H^\theta}{R}\left(\frac{1}{T_2} - \frac{1}{T_1}\right) \quad (18)$$

Results

The Adair's coefficients are fitted to the collection of ODC measurements by Severinghaus [18] at $pCO_2 = 0$ Pa and $pH_p = 7.4$, see Figure 2A and Table I. The dissociation coefficients of carboxylation are determined in close agreement with Bauer and Schröder using their data [24]; the resulting fit can be seen in Figure 2B, the coefficients are in Table II. The lumped acid dissociation coefficients for the side-chains pK_{hD} and pK_{hO} are estimated by optimization of Siggaard-Andersen's data [23] at DPG/Hbt = 0.84, pH = 6.5–8.0 and 37°C; the resulting fit can be seen in Figure 2C, and the coefficients complete Table II.

We conclude that the model also describes the ODC shifts by comparing with Naerea et al.'s [31] oxygen saturation measurements at different plasma pH and CO_2 levels, see Figure 2D. The recalculation of data from plasma pH_p to intracellular erythrocyte pH uses the equation $pH = 7.2464 + 0.796(pH_p - 7.4)$, as presented by Siggaard-Andersen and Salling [32].

The gas solubility as Henry's coefficient at different temperatures can be recalculated using the enthalpy of gas solution (-14 $kJ.mol^{-1}$ for O_2, and -20 $kJ.mol^{-1}$ for CO_2 [33]). If we assume that the examined hemoglobin of Matthew et al. [1] is at compatible conditions, but at a temperature of 30°C with $pK_{zD} = 7.53$, $pK_{zO} = 7.28$, $pK_{cD} = 4.77$ and $pK_{cO} = 5.20$ as plotted in Figure 2E, then the enthalpies of these reactions are -51, 8, 59 and -41 $kJ.mol^{-1}$.

Atha and Ackers measured the heat of hemoglobin oxygenation under conditions independent of carbon dioxide and Bohr protons and not including the oxygen heat of solution, coming to the value of 59 $kJ.mol^{-1}$ [34]. Using this value for each Adair oxygenation step, one can optimize other enthalpies to fit the Reeves data [25] measured at 19–43°C (Figure 2F). Resulting enthalpies are 59 $kJ.mol^{-1}$ for the deoxy and 127 $kJ.mol^{-1}$ for the oxy version of reaction h.
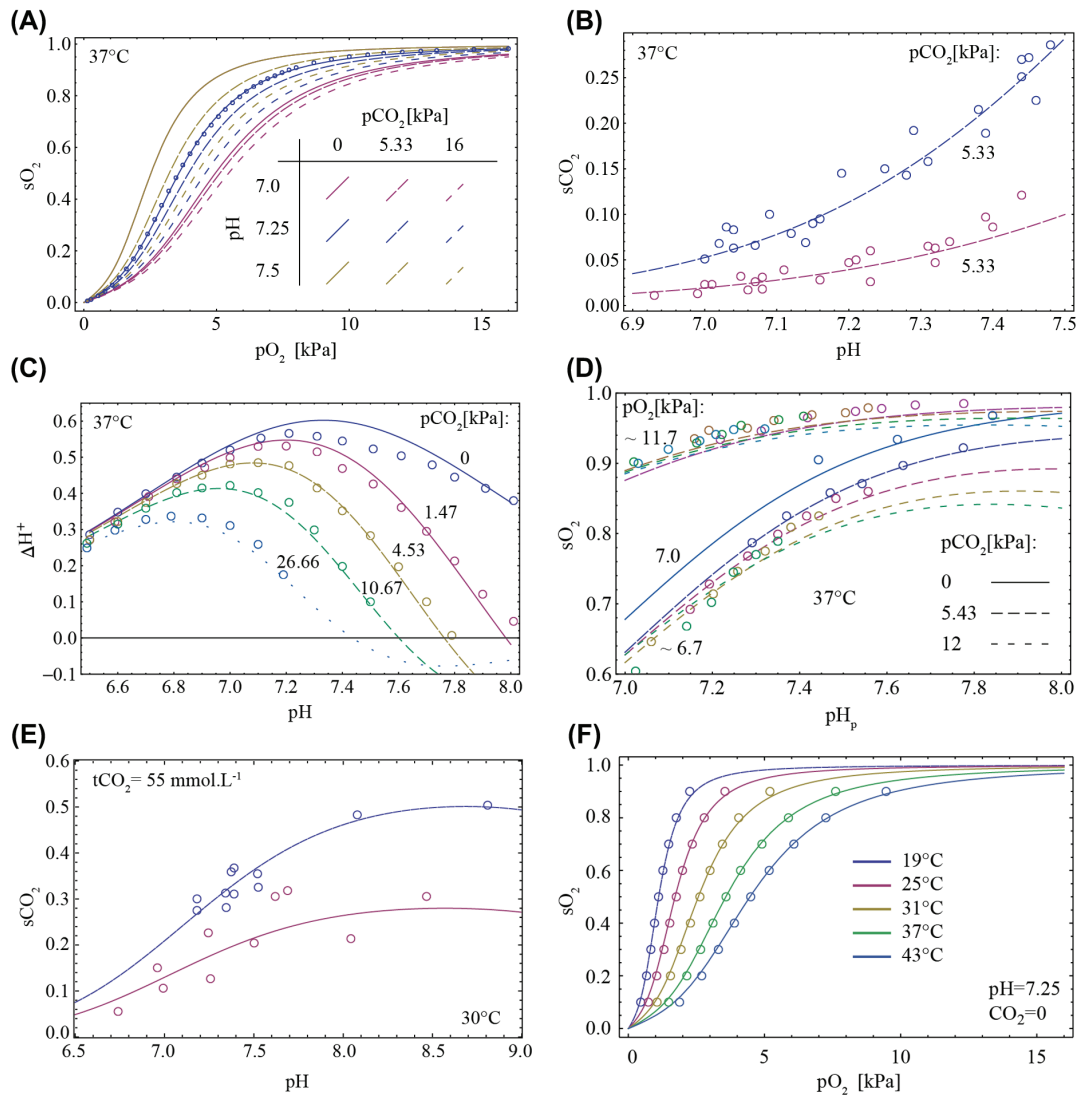
Figure 2. Model curves and measured data points. (A) Points are from Severinghaus's oxygen dissociation curve collection [18] at pCO$_2$ = 0 Pa, erythrocyte intracellular pH = 7.25 and temperature 37°C. Lines are sO$_2$ defined by Equation 15. (B) Carboxylation of hemoglobin measured and estimated by Bauer and Schröder [24]. The lines (Equation 7) are sCO$_{2D}$ and sCO$_{2O}$ at pCO$_2$ = 5.33 kPa. (C) Bohr protons released during oxygenation of one hemoglobin subunit. Dots are data measured by Siggaard-Andersen [23] in erythrolysate at 37°C, DPG/Hb$_t$ = 0.84. Lines are calculated from Equation 11 using coefficients from Table II. From top to bottom data are plotted for different pCO$_2$ = 0 kPa, 1.47 kPa, 4.53 kPa, 10.67 kPa and 26.66 kPa. (D) Naeraa et al.'s [31] oxygen saturation data comparison. The two groups of lines (Equation 15) are determined mainly by pO$_2$ around 6.7 kPa and 11.7 kPa. The small nuances in each group are caused by different pCO$_2$ changed from 0–12 kPa. (E) Matthew et al.'s [1] carbamination data measured at 30°C with constant content of all carbonates 55 mmol.L^{-1}. Fitted dissociation constants, which determine the lines, are used to estimate enthalpies of their reactions to be consistent with Bauer and Schröder [24]. (F) Reeves [25] oxygen saturation data at different temperatures. Enthalpies of reaction h and specific Adair oxygenation step enthalpy is estimated (lines) to fit the data (circles). This Figure is reproduced in color in the online version of *The Scandinavian Journal of Clinical & Laboratory Investigation*.

Discussion

Having a precise quantitative description of hemoglobin behavior is a crucial aspect in describing the behavior of whole blood, which has numerous uses in medicine today. It is important in areas such as blood gas analysis [15,34], the building of complex models [35], simulation for teaching purposes [36], or rebreathing-based methods for cardiac output estimation, which represent a more specific use [37]. For instance, the precision of the latter methods is crucially dependent on the exact calculation of the total amount of carbon dioxide in blood for various

Table I. Estimated form-specific Adair's coefficients [mol.m^{-3}] at 37°C.

K_1	K_2	K_3	K_4
0.0121	0.0117	0.0871	0.000386

Table II. Estimated acid dissociation coefficients at 37°C.

Reaction z	Reaction c	Reaction h
pK$_{zD}$ = 7.73	pK$_{cD}$ = 7.54	pK$_{hD}$ = 7.52
pK$_{zO}$ = 7.25	pK$_{cO}$ = 8.35	pK$_{hO}$ = 6.89

(abnormal) patient conditions, as has been recently pointed out [38].

This model offers a precise description of various phenomena that take place with hemoglobin, based on relatively simple starting points, such as competitive binding of H+ and CO_2 at valine-1 amino terminus or the law of detailed balance [30]. Even with a simple structure, it offers a remarkably good fit to the data of hemoglobin oxygenation, titration, and carbamination at different temperatures, as shown in Figure 2A–E. These can be calculated with any combination of oxygen, carbon dioxide and hydrogen ions defined as open system (lungs), where the partial pressures are equilibrated, and also in a closed system (tissues), where mass conservation laws and the total amount of substances take place, as was also modeled by Rees and Andreassen [39], among others.

The results of our model (Figure 2A–E) show strong nonlinear dependences between variables, which is in agreement with the known data [1,23–25,40]. Looking at Figure A, one can compare sets of ODCs, where each color represents a different pH. Various curves of each color represent ODCs for various levels of pCO_2 for a given pH. As can be seen, the effect of pCO_2 on the ODC is stronger at high (alkaline) pH, which is in agreement with the data [23]. Similarly, one can compare the curves within the sets of solid or dashed lines, where each set represents dissociation curves for various values of pH at a given level of pCO_2. The variation between the curves of each line type represents the Bohr effect for the given level of CO_2, this effect can also be appreciated from data of Figure 2C, which shows the average amount of released H^+ upon oxygenation of one hemoglobin subunit.

The model uses enthalpies to calculate temperature dependences of hemoglobin behavior (Figure 2F, E), which allows examination of the heat transfers during single chemical processes. For instance, binding of aqueous oxygen onto hemoglobin produces 30–40 kJ/mol of heat [41–44], and the same amount of heat is consumed by deoxygenation process in metabolically active tissues, thus helping to cool them down. When the hemoglobin model is used in the standard conditions of a large-scale Hum-Mod model [35], the resulting heat transfer due to the exothermy of the hemoglobin oxygen reaction is 4–7% of the total heat produced by muscle, which is in agreement with experimental results [41,43,44]. It is interesting to note that this heat transfer occurs without any increase in blood temperature.

The integration of chemical processes in a macromolecule requires a precise view into their underlying principles. Some physiologists use the elementary chemical equations [39], but do not implement the principle of detailed balance [30]. Other physiologists make empirically-based equations with a raw linear gradient approximation of possible combinations of model values [15]. We feel that it is almost impossible to see the problem as this type of black-box function with more than two inputs. Instead, it is better to have an integrated model of oxygenation, titration and carbamination.

Today, allosteric hemoglobin oxygenation models do exist that seem more in agreement with the structural knowledge of hemoglobin [12,45–47]. These models take into account two or more structurally different forms: relaxed and tensed. However, these models have so far been limited to hemoglobin oxygenation only. Our Adair-based model can explain not only oxygen and carbon dioxide saturation, but also their cooperation with acid-base buffering properties of hemoglobin. All three of these connected phenomena fit to measured data in physiological ranges.

As any work, the presented model has its limitations. First of all, it does not include the effects of changes in Hb tetramer conformations. Also the model could be extended with dependences on electrolytes such as chloride, 2,3-bisphosphoglycerate or other organic phosphates and their binding reactions, as many research studies show these interactions [48–51]. The next extension of this model could be performed by the integration of an intracellular red cell environment to calculate with phosphate acid-base buffers, and finally the membrane changes with blood plasma, where the chloride shift reaches a Gibbs-Donnan equilibrium and establishes chloride, bicarbonate and hydrogen ion activity ratios. Having an integrated model of blood gases and acid-base is crucial if we want the precise computational algorithms of the current state of a patient. These calculations could be used, for example, inside the next generation of medical devices to estimate not only blood properties, but also the connected properties of circulation [37] or metabolic functions [39].

In this article, we present a hemoglobin model that integrates O_2, CO_2 and H^+ binding. The model is not just empirical, but is based on sound theoretical principles, such as the competitive binding of CO_2 and H^+ on the valine-1 NH_2 terminus, the Bohr and Haldane effect [9,52] and on the principle of detailed balance. The principle of detailed balance is used for the first time in the Adair type of model. The advantages of this approach include explicit formulation of mass and energy conservation principles: The model accumulates substances and heat inside hemoglobin forms, making it very useful for integration in higher-scale dynamic models.

Acknowledgements

References

[1] Matthew JB, Morrow J, Wittebort RJ, Gurd F. Quantitative determination of carbamino adducts of alpha and beta chains in human adult hemoglobin in presence and absence of carbon monoxide and 2, 3-diphosphoglycerate. J Biol Chem 1977;252:2234–44.

[2] Perutz M. Species adaptation in a protein molecule. Mol Biol Evol 1983;1:1–28.

[3] Perutz M, Kilmartin J, Nishikura K, Fogg J, Butler P, Rollema H. Identification of residues contributing to the Bohr effect of human haemoglobin. J Mol Biol 1980;138:649–68.

[4] Rossi-Bernardi L, Roughton F. The specific influence of carbon dioxide and carbamate compounds on the buffer power and Bohr effects in human haemoglobin solutions. J Physiol 1967;189:1–29.

[5] Forster R, Constantine H, Craw MR, Rotman H, Klocke R. Reaction of CO2 with human hemoglobin solution. J Biol Chem 1968;243:3317–26.

[6] Stadie WC, O'Brien H. The carbamate equilibrium I. The equilibrium of amino acids, carbon dioxide, and carbamates in aqueous solution; with a note on the Ferguson-Roughton carbamate method. J Biol Chem 1936;112:723–58.

[7] Morrow J, Matthew J, Wittebort R, Gurd F. Carbon 13 resonances of 13CO2 carbamino adducts of alpha and beta chains in human adult hemoglobin. J Biol Chem 1976;251:477–84.

[8] Bohr C, Hasselbalch K, Krogh A. Concerning a biologically important relationship–the influence of the carbon dioxide content of blood on its oxygen binding. Skand Arch Physiolog 1904;16:402.

[9] Siggaard-Andersen O, Garby L. The Bohr effect and the Haldane effect. Scand J Clin Lab Invest 1973;31:1–8.

[10] Tyuma I. The Bohr effect and the Haldane effect in human hemoglobin. Jpn J Physiol 1984;34:205.

[11] Matthew J, Hanania G, Gurd F. Electrostatic effects in hemoglobin: hydrogen ion equilibria in human deoxy-and oxyhemoglobin A. Biochemistry 1979;18:1919.

[12] Monod J, Wyman J, Changeux J-P. On the nature of allosteric transitions: a plausible model. J Mol Biol 1965;12:88–118.

[13] Eaton WA, Henry ER, Hofrichter J, Bettati S, Viappiani C, Mozzarelli A. Evolution of allosteric models for hemoglobin. IUBMB Life 2007;59:586–99.

[14] Hill AV. The combinations of haemoglobin with oxygen and with carbon monoxide. I. Biochem J 1913;7:471.

[15] Siggaard-Andersen O, Siggaard-Andersen M. The oxygen status algorithm: a computer program for calculating and displaying pH and blood gas data. Scand J Clin Lab Invest 1990;50:29–45.

[16] Adair GS. The hemoglobin system VI. The oxygen dissociation curve of hemoglobin. J Biol Chem 1925;63:529–45.

[17] Dash RK, Bassingthwaighte JB. Erratum to: Blood HbO$_2$ and HbCO$_2$ dissociation curves at varied O$_2$, CO$_2$, pH, 2, 3-DPG and temperature levels. Ann Biomed Eng 2010;38:1683–701.

[18] Severinghaus JW. Simple, accurate equations for human blood O$_2$ dissociation computations. J Appl Physiol 1979;46:599–602.

[19] Christiansen J, Douglas C, Haldane J. The absorption and dissociation of carbon dioxide by human blood. J Physiol 1914;48:244–71.

[20] Perrella M, Bresciani D, Rossi-Bernardi L. The binding of CO2 to human hemoglobin. J Biol Chem 1975;250:5413–8.

[21] Mateják M, Kulhánek T, Šilar J, Privitzer P, Ježek F, Kofránek J. Physiolibrary-Modelica library for Physiology. 10th International Modelica Conference; 2014 March 12; Lund, Sweden: Linköping University Electronic Press; 2014. pp. 499–505.

[22] Mateják M. Physiology in Modelica. Mefanet J 2014;2:10–4.

[23] Siggaard-Andersen O. Oxygen-linked hydrogen ion binding of human hemoglobin. effects of carbon dioxide and 2, 3-diphosphoglycerate I. Studies on erythrolysate. Scand J Clin Lab Invest 1971;27:351–60.

[24] Bauer C, Schröder E. Carbamino compounds of haemoglobin in human adult and foetal blood. J Physiol 1972;227:457–71.

[25] Reeves RB. The effect of temperature on the oxygen equilibrium curve of human blood. Respir Physiol 1980;42:317–28.

[26] Kulhanek T, Matejak M, Silar J, Kofranek J. Parameter estimation of complex mathematical models of human physiology using remote simulation distributed in scientific cloud. Biomedical and Health Informatics (BHI), 2014 IEEE-EMBS International Conference on 1–4 June 2014; pp. 712–5.

[27] Sendroy J, Dillon RT, Van Slyke DD. Studies of gas and electrolyte equilibria in blood XIX. The solubility and physical state of uncombined oxygen in blood. J Biol Chem 1934;105:597–632.

[28] Maas A, Rispens P, Siggaard-Andersen O, Zijlstra W. On the reliability of the Henderson-Hasselbalch equation in routine clinical acid-base chemistry. Ann Clin Biochem 1984;21:26.

[29] Antonini E, Wyman J, Brunori M, Fronticelli C, Bucci E, Rossi-Fanelli A. Studies on the relations between molecular and functional properties of hemoglobin V. The influence of temperature on the Bohr effect in human and in horse hemoglobin. J Biol Chem 1965;240:1096–103.

[30] Sauro HM. Enzyme kinetics for systems biology. Future Skill Software (Ambrosius Publishing); 2011. pp. 20–1.

[31] Naeraa N, Petersen ES, Boye E. The influence of simultaneous, independent changes in pH and carbon dioxide tension on the in vitro oxygen tension-saturation relationship of human blood. Scand J Clin Lab Invest 1963;15:141–51.

[32] Siggaard-Andersen O, Salling N. Oxygen-linked hydrogen ion binding of human hemoglobin. Effects of carbon dioxide and 2, 3-diphosphoglycerate. II. Studies on whole blood. Scand J Clin Lab Invest 1971;27:361–6.

[33] Lide DR. CRC handbook of chemistry and physics. Boca Raton, FL: CRC Press; 2004.

[34] Atha DH, Ackers GK. Calorimetric determination of the heat of oxygenation of human hemoglobin as a function of pH and the extent of reaction. Biochemistry 1974;13:2376–2382.

[35] Hester RL, Brown AJ, Husband L, Iliescu R, Pruett D, Summers R, Coleman TG. HumMod: a modeling environment for the simulation of integrative human physiology. Front Physiol 2011;2.

[36] Kofranek J, Matousek S, Rusz J, Stodulka P, Privitzer P, Matejak M, Tribula M. The Atlas of Physiology and Pathophysiology: Web-based multimedia enabled interactive simulations. Comput Methods Programs Biomed 2011;104:143–53.

[37] Jarvis SS, Levine BD, Prisk GK, Shykoff BE, Elliott AR, Rosow E, Blomqvist CG, Pawelczyk JA. Simultaneous determination of the accuracy and precision of closed-circuit cardiac output rebreathing techniques. J Appl Physiol 2007;103:867–74.

[38] Sun X-G, Hansen JE, Ting H, Chuang M-L, Stringer WW, Adame D, Wasserman K. Comparison of exercise cardiac output by the Fick Principle using oxygen and carbon dioxide. CHEST J 2000;118:631–40.

[39] Rees SE, Andreassen S. Mathematical models of oxygen and carbon dioxide storage and transport: the acid-base chemistry of blood. Crit Rev Biomed Eng 2005;33.

[40] Imai K, Yonetani T. PH dependence of the Adair constants of human hemoglobin. Nonuniform contribution of successive oxygen bindings to the alkaline Bohr effect. J Biol Chem 1975;250:2227–31.

[41] Adair G, Cordero N, Shen T. The effect of temperature on the equilibrium of carbon dioxide and blood and the heat of ionization of haemoglobin. J Physiol 1929;67:288–98.

[42] Chipperfield J, Rossi-Bernardi L, Roughton F. Direct calorimetric studies on the heats of ionization of oxygenated and deoxygenated hemoglobin. J Biol Chem 1967; 242:777–83.

[43] Weber RE, Campbell KL. Temperature dependence of haemoglobin-oxygen affinity in heterothermic vertebrates: mechanisms and biological significance. Acta Physiolog 2011; 202:549–62.

[44] Weber RE, Fago A, Campbell KL. Enthalpic partitioning of the reduced temperature sensitivity of O2 binding in bovine hemoglobin. Comparat Biochem Physiol A: Molec Integrat Physiol 2014;176:20–5.

[45] Szabo A, Karplus M. A mathematical model for structure-function relations in hemoglobin. J Mol Biol 1972; 72:163–97.

[46] Brunori M, Coletta M, Di Cera E. A cooperative model for ligand binding to biological macromolecules as applied to oxygen carriers. Biophys Chem 1986;23:215–22.

[47] Henry ER, Bettati S, Hofrichter J, Eaton WA. A tertiary two-state allosteric model for hemoglobin. Biophys Chem 2002;98:149–64.

[48] de Bruin SH, Rollema HS, Janssen LH, van Os GA. The interaction of chloride ions with human hemoglobin. Biochem Biophys Res Commun 1974;58:210–5.

[49] Rollema HS, de Bruin SH, Janssen L, Van Os G. The effect of potassium chloride on the Bohr effect of human hemoglobin. J Biol Chem 1975;250:1333–9.

[50] Benesch R, Benesch RE, Yu CI. Reciprocal binding of oxygen and diphosphoglycerate by human hemoglobin. Proc Natl Acad Sci USA 1968;59:526.

[51] Bunn HF, Briehl RW. The interaction of 2, 3-diphosphoglycerate with various human hemoglobins. J Clin Invest 1970; 49:1088.

[52] Siggaard-Andersen O, Salling N, Nörgaard-Pedersen B, Rørth M. Oxygen-linked hydrogen ion binding of human hemoglobin. effects of carbon dioxide and 2, 3-diphosphoglycerate: III. Comparison of the Bohr effect and the Haldane effect. Scand J Clin Lab Invest 1972;29:185–93.